Chapter 46
ZnO Films Elaborated by D.C. Magnetron Sputtering

Lamia Radjehi, Linda Aissani, and Abdelkader Djelloul

Abstract The effect of the oxygen flow rate on the structural and optical properties of ZnO films was investigated. Zinc oxide films were deposited Si (100) wafers and glass substrate by a DC magnetron sputtering technique using Zn targets in an Ar/O_2 mixture atmosphere. The oxygen content was changed from 10 to 30 sccm. The different properties were analyzed by using XRD, SEM, profilometer, and UV-visible. The evolution of optical and structural proprieties as O_2 was investigated by XRD, Profilometer, FESEM and UV-visible. O_2 increasing lead to improve ZnO crystallinity in wirtzite phase and the films present (002) preferential orientation along the c-axis. ZnO films present a significant improvement in band gap that present an enlargement from 3.13 to 3.30 eV due to the crystallite size increase from 22 to 30 nm.

Keywords ZnO · Sputtering · Transparent thin film

46.1 Introduction

Zinc oxide is a well transparent conductive oxides (TCOs), which having lower material cost and easier to etch. Zinc oxide films are deeply studied since of attractive properties they have. As the ZnO hexagonal structure that mostly exhibits n-type semiconductor characteristics. Then its large optical band gap of 3.37 eV, high infrared reflectivity and transparency in the visible region and interesting electrical conductivity value of 103 Ω^{-1} cm^{-1} [1].

L. Radjehi (✉) · A. Djelloul
Laboratoire des Structures, Propriétés et Interactions Inter Atomiques (LASPI2A), Faculty of Science and Technology, Abbes Laghrour University, 40000 Khenchela, Algeria

L. Radjehi · L. Aissani · A. Djelloul
Matersciences Department, ABBES Laghrour-Khenchela University, P.O1252, 40004 Khenchela, Algeria

L. Aissani
Laboratory of Active Components and Materials, Larbi Ben M'Hidi University, 04000, Oum El Bouaghi, Algeria

Y. Chiba et al. (eds.), *Advances in Green Energies and Materials Technology*,
Springer Proceedings in Energy, https://doi.org/10.1007/978-981-16-0378-5_46

According to these interesting properties, zinc oxides can enter in several field applications. ZnO are attractive material choices for transparent electronics and solar cell applications [2]. In addition, ZnO films have different field such as gas sensor, cancer treatment [3] and piezoelectric films. In other hand, ZnO properties is strongly depend on the condition of deposition method. Moreover, different deposition techniques were used, such as the thermal oxidation method, reactive evaporation, sol–gel method, chemical depositions and reactive magnetron sputtering [4]. Magnetron sputtering is one of the greatest ZnO deposition method because it had an effective chemical composition control. It has high deposition rate with large deposition area [5].

In this study, zinc oxide films are fabrication by DC magneton sputtering MEP 600 Alacatel using a pure metal target of Zn on glass slides substrates. The results will be compared with those reported in the literature. Then a detailed exploration is given by analyzing its structural, morphological, chemical, and optical properties.

46.2 Experimental Detail

ZnO films with different O contents was deposited using DC reactive magnetron sputtering machine (Alcatel SCM600). High purity Zn (99.99%) circular targets of 20 cm in diameter were used. The substrates-targets distance was fixed at 140 mm to obtain films with uniform thickness and a good deposition rate. Films were deposited on Si (100) wafers (1×1 cm^2) and glass substrates. The coated Si wafers were used to measure the film chemical composition, thickness. The electrical intensity is 1A and the working pressure was carried out at 0.5 Pa. O_2 was varied between 10 and 30 sccm, however the Argon was fixed at 40 sccm. Thereafter, the substrates were cleaned in an ultrasonic bath of acetone and ethanol solutions for 10 min. Prior to the deposition procedure, the chamber was evacuated dawn to a low pressure of 2×10^{-5} Pa. The substrates and targets were cleaned by Ar ion etching for 10 min and surface oxide layers or impurities were removed. The cleaning step was performed with the following conditions.

By using X-ray diffraction (D8 advanced, with a CuK_α radiation source, 40 kV, 40 mA, and $\lambda_{Cu} = 0.154$ nm) the ZnO crystalline structure was analyzed. A profilometer (AltiSurf) was used to measure the films thickness. Field emission scanning electron microscope (FE-SEM-Hitachi-SU8030) was used to observe the cross-section, the film morphology and the chemical composition of the films. By using a Perkin Elmer UV–VIS Lambda 19 spectrophotometer in the 190–1200 nm spectral range was measured the transmittance of films synthesized on glass substrates.

46.3 Results and Discussion

Figure 46.1 shows the structure evolution of ZnO as function as oxygen flow rate that varied between 10 and 30 sccm. At low content of oxygen, weak peaks at 36.49° (002) and 43.47° (101) that assigned to Zn phase (JCPDS card N°#1–1238). In addition, other peak can be seen (100), (002), (103) and (004) has appeared at 31.77°, 34.42°, 62.86° and 72.56°. These peaks can be attributed ZnO phase (JCPDS Card N°#36–1451). From 15 to 30 sccm of oxygen, zinc phase has totally disappeared and ZnO phase becomes predominant and (002) peak revealed more intense. From 15 sccm, the peaks become more intense and sharper [5]. Therefore, O_2 increasing effectively affects the structure by enhancement of ZnO formation structure. Moreover, (002) ZnO peak position was moved towards higher diffraction angle. This can be explained by composition changing of films. This due to the oxygen insertion in Zn crystal lattice. Then, the lattice constants have changed and induce the compressive strain by voltage target decrease in sputtering process [6].

Figure 46.2 shows the elemental composition of the films obtained by EDS technique. oxygen increase lead to augmentation of O/Zn ratio until 1 and the film stoichiometry changed. At inferior O_2 value, ZnO film was under stoichiometric because of the existence of defect even oxygen vacancy that has produced during the deposition.

Figure 46.3 shows the cross section images of ZnO films deposited on Si (100) wafers under different O_2 flow rates. It has been see that films deposited at 10 sccm grew quickly and showed dense and rough with the appearance of micro-droplets in the free surface morphology that is due to compressive strain. According to Andres's SZM, the film structure corresponds to the zone II [7]. The surface present heterogeneous grain with spherical shape that is due to common interference of the intermediate Zn and ZnO phases (Fig. 46.1). Previous studies showed a similar morphology for the ZnO films deposited by DC unbalanced magnetron sputtering [8]. Between 25 and 30 sccm, the grain shape becomes round that is characteristic of the transition zone [7].

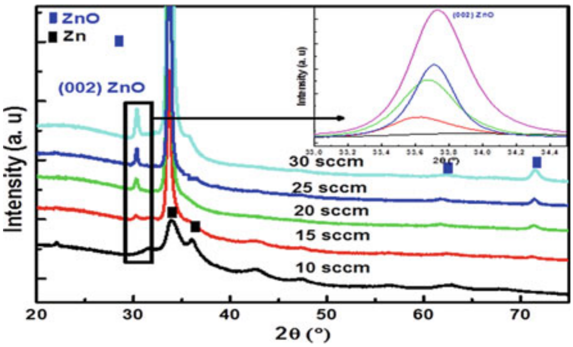

Fig. 46.1 XRD patterns of ZnO films at several oxygen flow rates

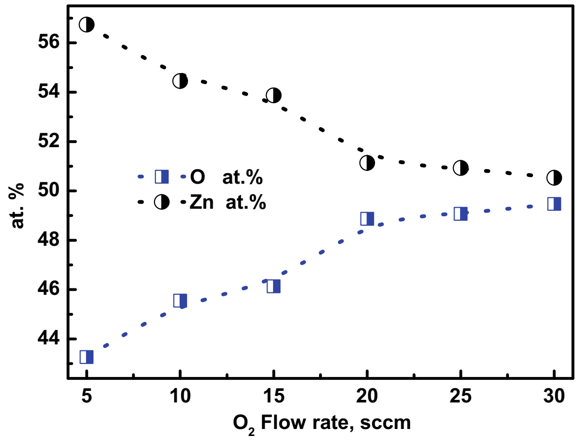

Fig. 46.2 Atomic percentage of ZnO films at different O_2 flow rates

ZnO transmittance was shown in Fig. 46.4 of film deposited at 10, 15, 25 and 30 sccm. A large absorption in UV region around 375 nm and a good transparency in visible wavelength was revealed for all samples. Oxygen increasing leads to improve in the films transmittance until 86% at 500 nm in visible region. Films deposited d 20, 25 and 30 sccm exhibit small size dispersion and there is band gap optimization up to 3.37 eV. Thus, at 10–15 sccm, present low transmittance because the films made by more free carriers.

The optical absorption coefficient (α) was estimated by the following transmittance relationship [8]:

$$\alpha = \frac{1}{d}\ln(T) \tag{46.1}$$

d is the thickness.

Furthermore, in addition, the relationship between E_g and the UV transmittance (T) was estimated as [9]:

$$\alpha h\nu = A\left(h\nu - E_g\right)^n \tag{46.2}$$

α is the absorption coefficient, h is Plank constant, hν is constant photon energy, n = 1/2 because ZnO is direct semiconductors.

Figure 46.5 presents the evolution of $(\alpha h\nu)^2$ versus hν data of ZnO films. The shift of the absorption edge to shorter wavelengths indicates that E_g becomes larger with O_2 increasing. The extrapolation of the linear part of $(\alpha h\nu)^2$ versus hν data (at $\alpha = 0$) allows us to calculate E_g. The films have an optical gap values of 3.14, 3.25 and 3.30 eV at 20, 25 and 30 sccm of O_2, respectively. J. Taucet al. found that, the increases in the O_2:Ar ratio, create stress films state that wave-length red shift compared to E_g of intrinsic ZnO (3.37 eV) [9]. Bedia et al. [10] reported that with

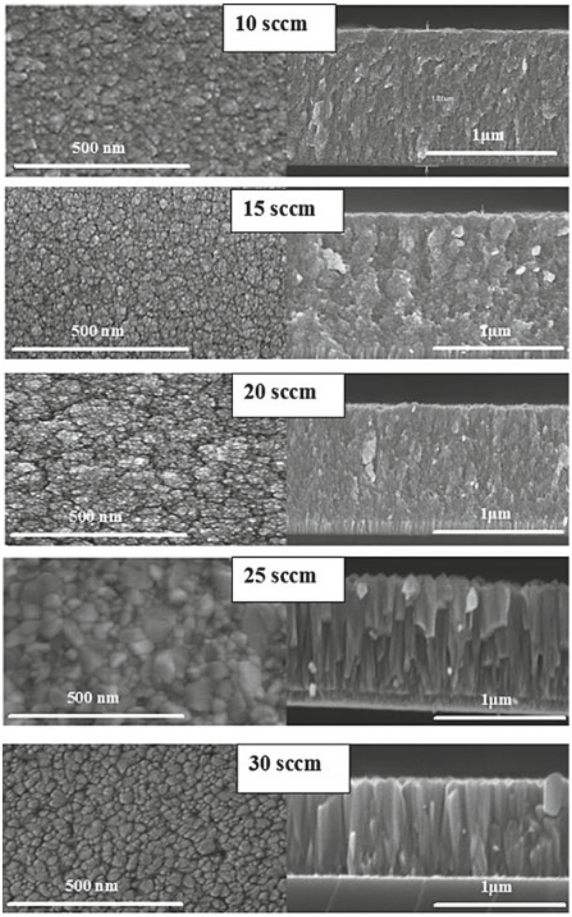

Fig. 46.3 SEM surface morphology and cross-section of ZnO films as function O_2

oxygen increasing the band gap improves and this is related to the grain size increase that is due to the band bending reduce in the grain boundaries [10]. In our work, the shift absorption edge of E_g from 3.14 (20 sccm) to 3.30 eV (30 sccm) may be assigned to grain size increasing.

In zinc oxygen films, the band gap is related to the lower carrier density, which is due oxygen vacancies appears in the structure. Moreover, increasing of the band gap is linked to oxygen vacancy concentration [11].

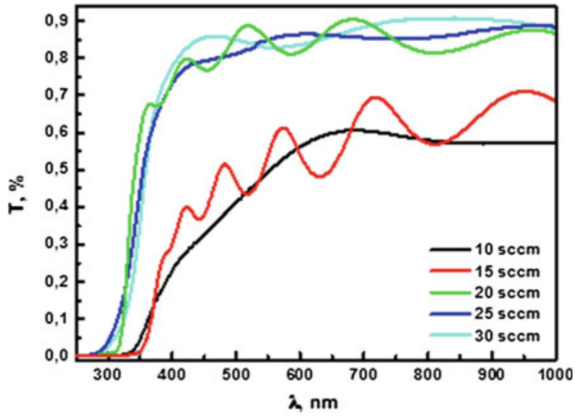

Fig. 46.4 Transmission as function oxygen for zinc oxide films deposited on glass substrates

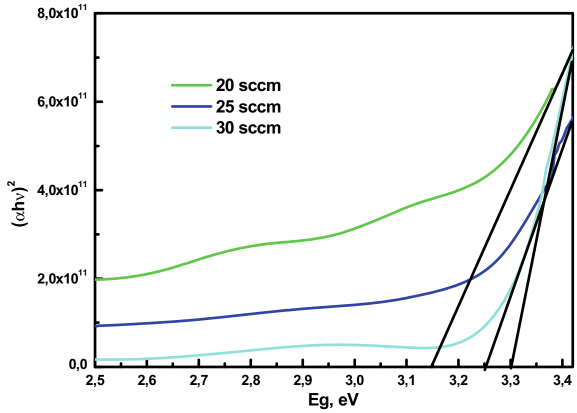

Fig. 46.5 E_g as function oxygen for zinc oxide films deposited on glass substrates

46.4 Conclusion

This article focuses on the evolution of the different properties of ZnO films as function oxygen flow rate. An improvement in ZnO structure even the band gap becomes larger with O_2 increasing. The films were deposited using the D.C magnetron sputtering process. At 10 sccm, the film morphology show a dense and columnar structure with a mixture of Zn and ZnO. From 30 sccm, film structure grow to be spherical grain with (002) ZnO preferential orientation. Best optical and structural properties was shown for the film deposited at 30 sccm. Thus, the optical transmittance and band gap increase to reach a values 88.7% (at 500 nm) and 3.30 eV, respectively. As result of O_2 increasing the band gap enlarged this is due to oxygen vacancy decrease.

References

1. Z.L. Wang, Zinc oxide nanostructures: growth, properties and applications. J. Phys.: Condens. Matter **16**, 829–858 (2004)
2. B. Wacogne, M.P. Roe, T.A. Pattinson, C.N. Pannell, Effective piezoelectric activity of zinc oxide films grown by radio-frequency planar magnetron sputtering. Appl. Phys. Lett. **67**(12), 674–1676 (1995)
3. K. Rekha, M. Nirmala, M.G. Nair, A. Anukaliani, Structural, optical, photo-catalytic and antibacterial activity of zinc oxide and manganese doped zinc oxide nanoparticles. Phys. B **405**(15), 3180–3185 (2010)
4. L. Znaidi, S. Benyahia, C. Sanchez, A.V. Kanaev, Oriented ZnO thin films synthesis by sol-gel process for laser application. Thin Solid Films **428**(1–2), 257–262 (2003)
5. X. Zhang, S. Ma, F. Liu, X. Tang, J. Liu, Q. Zhao, Effects of substrate temperature on the growth orientation and optical properties of ZnO:Fe films synthesized via magnetron sputtering. J. Alloys Compound **574**, 149–154 (2013)
6. D. Thomas, S.C. Vattappalam, S. Mathew, S. Augustine, Studies on effect of oxygen flow rate in textured grain growth of ZnO thin films. Mater. Sci. Eng. **73**, 1–5 (2015)
7. L. Aissani, M. Fellah, C. Nouveau, M. Abdul Samad, A. Montagne, A. Iost, Structural and mechanical properties of Cr–Zr–N coatings with different Zr content. Surf. Eng. **33**, 1743–2944 (2017)
8. P.S. Silva, P. Edinéia, S. Schmitz, A. Spinelli, J.R. Cracia, Electrodeposition of Zn and Zn–Mn alloy coatings from an electrolytic bath prepared by recovery of exhausted zinc–carbon batteries. J. Power Sources **210**, 116–121 (2012)
9. J. Tauc, *Amourphous and Liquid Semiconductor* (Plenum Press, 1974)
10. A. Bedia, F.Z. Bedia, M. Aillerie, N. Maloufi, B. Benyouce, Morphological and Optical properties of ZnO thin films prepared by spray pyrolysis on glass substrates at various temperatures for integration in solar cell. Eng. Procedia **74**, 529–538 (2015)
11. H. Liu, F. Zeng, Y. Lin, G. Wang, F. Pan, Correlation of the oxygen vacancy variations to the band gap changes in epitaxial. Appl. Phys. Lett. **102**, 181908 (2013)